

ORIGINAL ARTICLE

Magnetic resonance imaging used for the evaluation of water presence in wood plastic composite boards exposed to exterior conditions

MAREK GNATOWSKI¹, REBECCA IBACH², MATHEW LEUNG¹, & GRACE SUN¹

¹Polymer Engineering Company, Burnaby, BC, Canada and ²USDA Forest Service Forest Products Laboratory, Madison, WI, USA

Abstract

Two wood plastic composite (WPC) boards, one experimental and one commercial, were exposed to exterior conditions and evaluated non-destructively using a clinical magnetic resonance imaging (MRI) unit for moisture content (MC) and distribution. The experimental board was exposed in Vancouver, British Columbia, for more than 8 years, and the commercial board was exposed near Hilo, Hawaii, for 2 years. Both boards were characterized in terms of wood content, density, water uptake properties and voids content. The experimental board was additionally destructively analysed for water absorption of the WPC and MC calculated based on the wood content for verification of MRI results. MRI detected the presence of free water and its distribution in both of the WPC boards. Fibre saturation in the experimental board was found to be about 22–24%, in comparison to 25–30% present in most wood species. There was good correlation between the detection of free water by MRI and by destructive testing. Magnetic resonance images showed various major points of water entry in the WPC boards such as the support area, the cut ends, the dripping edge and the sides of the boards. For the experimental board, significant water entry also occurred at the upper exposed surface.

Keywords: *Computed tomography, exterior exposure, magnetic resonance imaging, moisture content, water absorption, wood plastic composite, void analysis*

Introduction

Industry and academia experience related to moisture absorption and distribution in wood plastic composite (WPC) materials is limited and controversial. ASTM standards D7031 and D7032 (ASTM International 2013c, 2013d) recommend the testing of WPC water absorption (WA) based on a method developed for evaluating the properties of wood-based fibre and particle panel materials – D1037 (ASTM International 2013b). WPC decking boards or railings tested according to this method have frequently showed low WA in the range of 1% or below.

WA, however, significantly influences the performance and durability of WPC products. Excessive water content and moisture cycles cause composite profiles to warp (Morris and Cooper 1998) as well as decrease in mechanical properties (Kaboorani *et al.* 2007, Morrell *et al.* 2009). Water content in wood that is close to or exceeds 25% makes the material susceptible to decay. There are

several publications that have reported development of decay in WPC materials found in both laboratory studies and during field inspections (Schmidt 1993, Morris and Cooper 1998, Laks and Verhey 2000, Mankowski and Morrell 2000, Clemons and Ibach 2002, Ibach and Clemons 2002, Pendleton *et al.* 2002, Verhey *et al.* 2003, Laks *et al.* 2005, 2010). WA varies in WPCs and depends on material composition, such as wood content and species, particle size of wood flour and coupling agents used, etc. Processing conditions such as compression moulding, injection moulding or extrusion also give shaped objects different WA characteristics (Korte and Hansmann 2005). WPCs have a thermoplastic-rich surface layer that is created during their processing (through extrusion, compression moulding or injection moulding) that produces high levels of water repellence (Clemons and Ibach 2004). In the case of extruded profiles, extrusion conditions such as the type of extruder or screw

rotation speed also influence WPC properties, including WA (Englund and Olson 2007, Yeh and Gupta 2007).

Most of the world's manufacturing of WPC products are related to the decking and railing market in the USA. Installed decking boards and railing profiles are exposed to harsh exterior environments from the subzero temperatures of Arctic Alaska, to the hot desert climate of Arizona, to the sub-tropical wet climates in Florida and Hawaii. Regardless of the significant commercial use of this type of composite and the importance of WA influencing durability and mechanical properties, the knowledge of WA and distribution in WPC decking boards and railing exposed to exterior service conditions is still very limited. It was found during laboratory immersion of WPC samples that although commercial WPC absorbs water at a much slower rate than wood, a significant amount of moisture could still enter those materials after prolonged exposure. Most of the water was detected near the sample surface (Wang and Morrell 2004). Manning and Ascherl (2007) conducted testing of WA and distribution in commercial decking boards exposed in Hawaii for several years. A significant quantity of water was detected when cut samples were returned to the laboratory and tested destructively. A study related to WA and distribution in extruded experimental composite boards that matched the WA of some commercial materials was also reported (Gnatowski 2005, 2009). Full-sized boards were exposed in Vancouver, British Columbia, and Hilo, Hawaii, and tested by a destructive method combined with drying. It was found that a significant quantity of water could enter the WPC boards during exterior exposure. Cut ends of the boards and the upper surfaces were found to be the most vulnerable to water entry, but increased moisture content (MC) was detected in the whole board cross-section. No details of water distribution could be gathered due to the limitations of the method used.

It is known that water can be present in wood in different forms (Telkki *et al.* 2013). Bound water is absorbed by the cell walls of wood lumens until fibre saturation occurs. The limitation in bound WA is the number of free polar sites (mainly hydroxyls) in the wood structure, and when all of these sites have taken up water, fibres reach their saturation point. According to ASTM Standard D9, the fibre saturation point is the MC at which the cell walls are saturated with water (bound water) and no water is held in the cell cavities by capillary forces; it usually is taken as 25–30% MC, based on weight (ASTM International 2013a). When the amount of water in wood increases above the saturation point, it

becomes collected in the lumens and such water becomes free or mobile water. Some of this water gets into the pores of the fibres without direct bonding to their surface, in the form of micropore water.

Bound and free water in wood has been extensively investigated using nuclear magnetic resonance (NMR) techniques; however, much less attention has been paid to this phenomenon in WPCs. Using NMR relaxation time distributions, the fibre saturation point, hydroxyl site content and the amount of micropores were determined in wood (Telkki *et al.* 2013). They found that below 0°C the pine and spruce sapwood 'free water' was frozen and its signal disappeared, but in contrast, the 'bound water' remained unfrozen. Above 0°C 'free water' peaks dominated and some exchange occurred between the 'free water' and 'bound water' pools. In wood, the amount of bound water depends on the number of active sites available. In WPC wood flour particles, the number of available active sites may be changed to some degree, due to the chemistry, processing and composite structure of the material. The presence of bound water in WPC has been evaluated using tetrahertz time-domain spectroscopy (Jördens *et al.* 2010). There are, however, limited data in literature with respect to free and bound water in WPC materials (Lulianelli *et al.* 2010).

Magnetic resonance imaging (MRI) seems to be a suitable method of non-destructive evaluation for WPC since it is already a well-established method for imaging mobile water in wood, with the first work in this field published over 25 years ago (Hall *et al.* 1986, Wang and Chang 1986). A detailed review of literature in the field of application of the NMR technique for wood-related research was prepared by Bucur (2003) and more recently by Stenstrom *et al.* (2009). MRI was found to be a versatile application in wood science. For example, MRI was used by Muller for the early detection of fungal decay based on findings of increased MC in wood samples (Muller *et al.* 2001). Olson *et al.* (1990) applied MRI to measure MC and moisture distribution in wood during the drying process. A specially designed, portable MRI system was used in the forest for *in situ* analysis of living trees (Jones *et al.* 2012). MRI was also used for the evaluation of thermally modified wood (Telkki *et al.* 2010). Plants other than wood, for example broccoli, were also imaged using an MRI system to find moisture distribution during the drying process (Jin *et al.* 2011).

The contrast of a conventional MRI system image depends on the concentration of protons and length of signal lifetime. Bound water has a short signal

lifetime in the order of 1 ms, whereas free water present in wood lumens has this parameter in the range 10–100 ms (Araujo *et al.* 1992, MacMillan *et al.* 2011). The free water present in wood above the fibre saturation point, which is required to initiate decay, was our interest in this study and as such, a conventional MRI system, such as the one used in a clinical application, was well suited for our purposes. Bound water and other protons present in wood or a synthetic polymer structure would not be visible during the imaging experiment (MacMillan *et al.* 2011). The structure of WPC differs from solid wood or plants that were imaged by MRI and described in literature in that the composite involves small wood flour particles that are water absorbers and carriers comparable to the spatial resolution of many MRI systems. These particles are usually dispersed in or at least partially saturated by a hydrophobic polyethylene matrix that has practically no WA. The degree of polymer saturation of wood lamella during the manufacturing of WPCs depends on the wood species used (Gacitua and Wolcott 2009).

The location of free water is dependent on WPC microstructure. Such microstructure and the presence of voids in WPCs have been investigated using Scanning Electron Microscopy (SEM) image analysis (Gacitua and Wolcott 2009). Another method for non-destructive examination of materials is modern micro- or nano-computed tomography (CT) technology. Micro X-ray CT scans were used in the past by several researchers to image the WPC structure (Wang *et al.* 2007, Cheng *et al.* 2010, Defoirdt *et al.* 2010, Evans *et al.* 2010, Kastner *et al.* 2012). However, void size and content in such composites were not evaluated. Recently, new developments in micro X-ray CT inspection allowed for more effective examination of WPCs, with better resolution and distinction of materials with similar densities, such as that of wood and synthetic resins. Three-dimensional (3D) image analyses with determination of void size and content at the micron level became possible.

The objective of the research described in this article is the development and demonstration of MRI as a non-destructive method that allows the detailed examination of WPC boards or railing profiles for moisture concentration and distribution. Of particular interest is the MC in the wood of the composite at around 25% and above, as this moisture level makes the composite vulnerable to decay. This has to be distinguished from WA in the entire composite sample, as only a portion of the composite is composed of wood. Establishing such a non-destructive method for testing moisture in WPC allows further examination of decking boards that

show symptoms of decay, as well as new information to be gained about favourable conditions for decay in this type of composite. Evaluation of MC also required the development of a method for testing wood content in WPC for calculation of MC based on the known WA in the composite. This work also involved characterization of the tested materials in respect to void size and concentration, as such voids could act as reservoirs for free water detected by MRI.

Materials and methods

Chemicals (decahydronaphthalene, 2,2-methylene-bis (6-tert-butyl-4-methylphenol, isopropyl alcohol, acetone) were purchased from Aldrich Chemical Company, Milwaukee, Wisconsin.

Two types of WPC materials were evaluated:

- (1) Experimental
- (2) Commercial

Experimental WPC was formulated based on earlier research and matched the WA characteristics of some commercial WPC decking products available on the North American market around 2002. The composition of this WPC board can be found in Table I. The boards were made to match the manufacturing process, dimensions and WA of some selected commercial deck boards. Experimental WPC #106 was extruded as nominal 2.5 cm (1") thick by 15.2 cm (6") wide boards by the Composite Materials and Engineering Laboratory of Washington State University in Pullman, Washington. This was done as part of a larger experiment, and the labelling of experimental WPC #106 reflects the original identifications used. Raw materials were carefully batch blended and processed using a Milacron (Mount Orab, Ohio) 55 mm conical counter-rotating twin screw extruder with Strandex (Madison, Wisconsin) die. The melt temperature was 180°C (375°F). Boards were initially cut into

Table I. Composition of experimental WPC.

Component	Composition (wt%)
Wood flour pine ^a	67
HDPE resin ^b	29
Lubricants ^c	3
Talc ^d	1

^aWood flour grade 2020 (American Wood Fibers, Maryland).

^bHigh-density polyethylene B-53 35H flakes (Solvay, Brussels, Belgium).

^cBlend of zinc stearate (Ferro Chemical, Mayfield Heights, Ohio), 67 wt%; EBS Wax GE Specialty Chemicals, Singapore), 33 wt%.

^dNicron 403 (Luzenac America Inc, Three Forks, Montana).

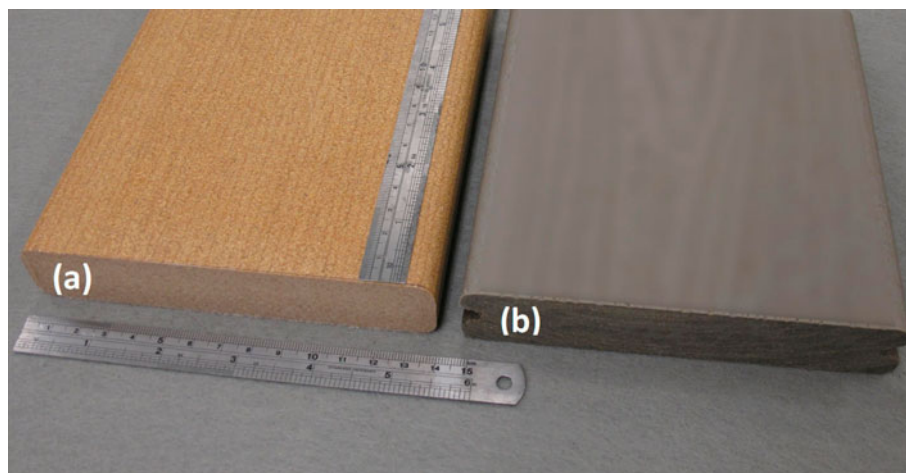


Figure 1. (a) Experimental and (b) commercial WPC boards used for testing.

0.915 m (3') long pieces. Each piece was marked with the date of manufacturing, formulation number and sequential board number. These experimental boards were manufactured in April 2003. A segment of the experimental board tested is shown in Figure 1.

Commercial boards were purchased at a building materials outlet and shipped to the exposure site in Hawaii. The board of interest was purchased in 2010 and had similar dimensions to the experimental board mentioned earlier, with nominal 2.5 cm (1") thickness, 15.2 cm (6") width and 0.915 m (3') length. The board had grooves on both sides for inserting fasteners, and the upper side was covered by a plastic coating, most likely coextruded with the WPC board body (capping). Segments of the tested board are shown in Figure 1.

Both reference unexposed experimental and commercial boards were analysed in the laboratory to identify composite density, board WA and MC in wood, as well as void size and content. The commercial board was further analysed for wood content, particle size and distribution, as well as for the characterization of the plastic resin used in extrusion of the WPC and its protective coating.

Density and WA of experimental and commercial WPC boards

Both experimental and commercial boards were tested for density and WA, following the recommendations of ASTM standards D7031/D1037. The density of oven-dried samples was measured in triplicate using nominal 2.5 cm (1") cubed samples. Two specimens each with nominal 15.2 cm (6") length, 15.2 cm (6") width and original thickness were obtained from the experimental and commercial boards. All original board surfaces were

maintained, including the fastening grooves on the commercial board. Specimens were conditioned for 2 days at 20°C and 65% relative humidity prior to immersion in distilled water maintained at the same temperature. After 24 hours of water immersion, specimens were dried in an oven at 103°C for 2 days. WA of the board samples and corresponding MC based on the wood content was determined with respect to total water uptake from storage of the boards and after the 24-hour water immersion. WA after 24 hours of water immersion was additionally expressed as an overall percentage and as the amount of water having entered the composite during the 24-hour water immersion per square centimetre (or square inch) of its exposed WPC surface. This was done to compensate for the differences in WA between the experimental and commercial boards due to the lack of an extruded capping layer between the former and the latter. The capping on the commercial board is a water-imperious protective coating, which covers about 40% of the sample surface. WA was calculated based on the weight of the whole sample, while MC was calculated based on the wood weight in the samples evaluated. The WA and MC properties of the experimental and commercial boards were compared to that of a solid wood board (Western Maple) and to a rectangular-shaped segment of polyethylene plastic with dimensions similar to the WPCs, both tested in a similar manner.

CT imaging of experimental and commercial boards

Micro X-ray CT was conducted at the GE Inspection Technologies, LP Customer Solutions Center in San Carlos, California. A GE phoenix|X-ray nanotom m (GE Sensing & Inspection Technologies GmbH; Wunstorf, Germany), equipped with a

180 kV, high-power nanofocus X-ray tube and DXR 500L flat-panel detector, was used. This instrument is known not only for its high scanning resolution (resolving features as small as 200 nm) but also for the high dynamic range of the detector (>10,000:1). This provides high-contrast resolution, or the ability to resolve and differentiate between materials of similar densities.

One specimen with nominal dimensions, 19 mm (0.75") × 19 mm (0.75"), and original thickness was taken from each of the experimental and commercial boards at a random location near the middle of the board. These samples were attached with hot melt glue to thermally stable, clear-fused quartz rods (Technical Glass Products, Inc.; Painesville, OH) for imaging. Both samples were CT scanned using a 16 μm voxel size and 6.250X magnification, X-ray parameters were also standardized (750 ms timing, 3 averages, 1 skip, 90 kV, 250 μm and 1100 images). The entire geometry of the samples was imaged with two-dimensional (2D) acquisition images taken during 360° rotation of the sample. *VGStudio Max 2.2* acquisition and reconstruction software (GE Sensing & Inspection Technologies GmbH) was used for the acquisition and 3D reconstruction of CT images, respectively. *VGStudio Max 2.2* (Volume Graphics, GmbH) was used for viewing and analysis of the reconstructed volumes. Two-dimensional slice images of selected internal cross-sections were obtained.

In addition, for each sample, three sub-volumetric regions with a nominal 50 mm³ volume were randomly selected for void analysis. The defect detection module in *VGStudio Max 2.2* detected the presence, size and distribution of voids in each selected region and provided the void percentage for each sub-volume. The average void volume for each sample tested was calculated based on the data obtained from the three sub-volumes.

Additional characterization of the commercial board

Wood content of the commercial board was analysed by dissolving about a 1 g sample of the oven-dried composite in decahydronaphthalene containing 1% of the antioxidant 2246 [2,2-methylenebis (6-tert-butyl-4-methylphenol)]. This sample was placed in a 400 mesh stainless steel pouch and immersed in a 500 ml flask with 250 ml of solvent. The dissolution process was carried out under reflux at the solvent boiling temperature of about 168°C for 8 hours. The pouch with the remaining wood was then removed from the flask and briefly rinsed with fresh, hot decahydronaphthalene solvent. The excess solvent was absorbed by patting the pouch with paper towel, and it was then dried to constant weight, initially

overnight in the fume hood and finally in an oven at 103°C. A Mettler AC50 analytical balance (Mettler Toledo, Ohio) with accuracy of 0.1 mg was used for weighing. The pouch was opened after drying and weighing was completed, and the remains of the wood were inspected for potential contamination, including fragments of undissolved plastic and contaminants other than wood, such as mineral fillers (if any), using a Leica MZ 12 stereoscopic microscope. The amount of wood in the sample was found from the weight difference between the weight of the dry pouch with wood remains and the weight of the empty pouch. Additionally, about 1 g of WPC sample was ashed at 550°C and 900°C to find the quantity of inorganic pigments and fillers present.

Resins used in manufacturing the composite were characterized based on Fourier transform infrared (FTIR) spectra and differential scanning calorimetry (DSC) thermograms. For FTIR spectrophotometry, a sample of composite was dissolved in a similar way as the analysis of wood content and the resulting decahydronaphthalene solution was filtered while it was still hot, using a 15 cm diameter grade 202 filter paper (Whatman Reeve Angel) to remove insoluble contaminations. The polymer was precipitated from one portion of the filtered solution by the addition of half a portion of *n*-hexane and filtered again after cooling. The polymer was then washed with isopropyl alcohol followed by acetone and air dried for 24 hours prior to FTIR spectroscopy analysis. For the commercial board, a random sample was cut from the board protecting coating (capping) for resin characterization. An Avatar 370 FTIR spectrometer controlled by Omnix software (Thermo Nicolet) was used with Split Pea attachment for acquisition of the FTIR spectra. A DSC 7 instrument controlled by Pyrus software (Perkin Elmer) was employed for thermal analysis using either a mixture of small samples of WPC cut from 10 randomly selected board areas or samples cut from the protective coating. The thermal analysis experiment conditions were set up according to standard ASTM D3418.

The thickness of the plastic coating was measured on the photomicrographs of the image of the board cross-section made with a Leica MZ 12 microscope equipped with Leica DFC 320 digital camera (Singapore). The areas used for imaging were selected based on an inspection of the whole cross-section, and a representative area for coating thickness measurement was chosen. An ImagePro Express image analysis programme was employed for measurements.

Wood flour particles from the commercial board were recovered after dissolving polyethylene from the WPC material as described earlier and were characterized with respect to their aspect ratio, size

and size distribution. Characterization was conducted by measuring images of a representative sample of the particles captured using a Leica MZ 12 microscope equipped with a DFC 320 digital camera and ImagePro Express image analysis software. Ten images with a total of 1323 randomly selected particles, with a minimum 0.008 mm^2 size cut-off, were used. Assumptions were made that the width and thickness of the particles, not visible on the images, were identical and that the aspect ratio of the particles was not dependent on particle size. The aspect ratio was calculated from the measurement of 27 of the largest particles found on the images.

WPC boards exposure, samples collection and inspection

The experimental board was tagged for identification (#106) and then was exposed in Vancouver, British Columbia, from July 2003 to December 2011. The board was oriented in a horizontal position and fastened using screws in two places to the treated wood frame constructed about 305 mm (1') above the ground. The exposure site was located in shadow under a large Douglas Fir tree. Contact with the frame wood was 38 mm (1.5") wide across the WPC board. Vancouver has an annual average precipitation of 1118 mm (44") and an average annual temperature of 11°C with average minimum around 2°C and average maximum around 23°C . Just before MRI, the board was unscrewed from the frame, the metal identification tag was removed and the board was wrapped tightly in several layers of plastic film. Above freezing temperatures were observed during the period of sample collection. MRI was conducted within a few hours of board removal from the field to avoid drying and water migration.

The commercial board was tagged for identification (#1841) and exposed in shadow under an Albizia tree near Hilo, Hawaii, from November 2010 to November 2012. The board was also exposed in a horizontal position and fastened with two screws to a frame made from treated wood, similar to how it was done in Vancouver. The board was installed about 914 mm (3') above the ground. Hilo has an average annual precipitation of 3200 mm (126") and average daytime annual temperatures with highs around 27.2°C (80.9°F) and lows around 19.3°C (66.8°F). The site was briefly inspected a year later in 2011, and a sample was cut about 100 mm from the exposed edge for an initial evaluation. In November 2012, a second sample was collected. This sample contained the area where the board support and screw hole were located near the centre of the width of the board. The sample was marked, carefully wrapped in several layers of plastic film and couriered overnight to the PEC laboratory. Upon

arrival, the sample was immediately placed in a freezer at a temperature of -20°C before imaging. MRI was conducted in February 2013. The wrapped sample of commercial WPC board was thawed for about 4 hours at room temperature prior to MRI evaluation.

As mentioned, sister samples of both experimental and commercial WPC boards, which had been stored in a warehouse with no contact with exterior conditions, were used for the characterization of the materials.

Destructive testing for WA and MC

The wrapped experimental board #106 was placed in a freezer directly after MRI. Based on MRI results of the board evaluation, three areas were selected for destructive testing of WA in the composite as shown in Figure 2. Area 1L – $18 \times 27.5 \times 58 \text{ mm}$ ($0.71'' \times 1.08'' \times 2.24''$) in size was adjacent to the cut edge of the board and included holes from the removed tag screw. Area 2C – $27.5 \times 38 \times 51 \text{ mm}$ ($1.08'' \times 1.50'' \times 2.00''$) in size was located in the centre of the board and was used to find water distribution changes with board thickness. Area 3C was selected as it was in contact with the wooden support platform during exposure. The width of the sample, 38 mm (1.50"), was the same as the supporting beam. The fastening screw hole was near the centre

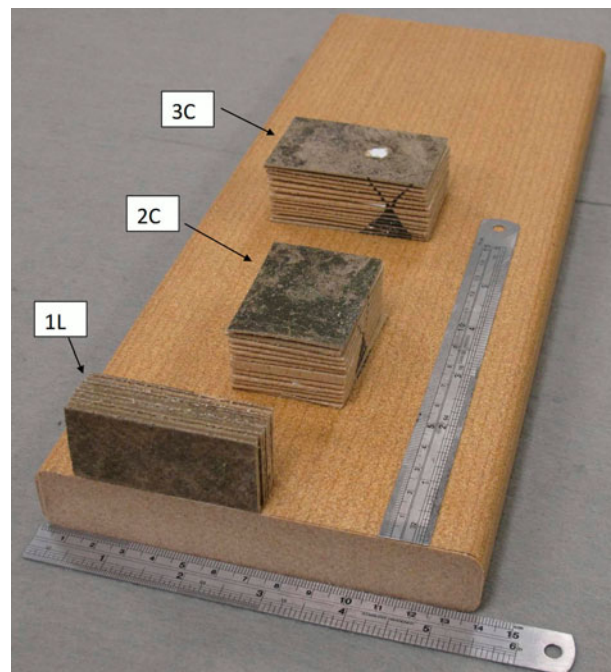


Figure 2. The respective locations and orientations of samples cut from the experimental board and used for destructive testing, including determination of WA and MC and distribution.

of the sample. This sample had a thickness of 27.5 mm (1.08") and a length of 62 mm (2.44").

Samples were further cut using a band saw into thin wafers, with a target nominal thickness of 1 mm (0.039") as shown in Figure 2. By wafering and drying wafers at 103°C, WA and MC distribution at a distance from the cut edge or through the thickness of the board were found. To identify the distance of the locations of each wafer from the board surface, the thickness of each dry wafer was measured at five points and the average thickness was calculated. Thicknesses of each wafer were added together and subtracted from the measured dry thickness of the tested board. This difference was divided by the number of cuts used to waferize the sample for calculation of the saw kerf, which was determined to be approximately 1 mm (0.039"). With knowledge of the average wafer thickness and kerf, the distance of each wafer's centre from the board surface was calculated. Special care was taken to avoid moisture dislocation or loss during handling. Cut specimens were instantly sealed in preweighed plastic bags for further handling and initial weight measurements without moisture loss.

The reference sample of experimental WPC board #106 was also tested for WA and MC according to ASTM D7031/D1037, by immersion in water for 24 hours and drying in an oven at a temperature of 103°C ± 2°C to constant weight. MC was calculated based on the known wood content.

Magnetic resonance imaging

MRI of the boards was carried out by the Canadian Magnetic Imaging Laboratory in Vancouver, British Columbia. A clinical Siemens Magnetom Espree 1.5 Tesla model TIM [32 × 8] MRI system (Siemens, Germany) was employed. This instrument provided

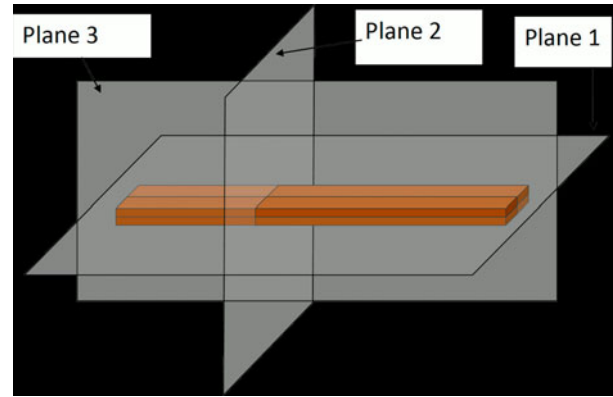


Figure 3. Position of MRI planes on the WPC boards – Plane 1: 4 mm or 8 mm slice in the horizontal plane; Plane 2: 8 mm slice in vertical plane perpendicular to the board length; Plane 3: 8 mm slice in a vertical plane parallel to the board length.

an image zone with field of view (FOV) 320 mm (about 12.6") along the WPC board length. The image matrix 521 × 521 corresponded to the spatial resolution of about 0.55 × 55 mm. For image acquisition, flash gradient echo sequence was employed with an echo time of 2.7 ms and repetition time of 6.1 ms. The majority of the scans were performed using the following slicing thickness shown in Figure 3: Plane 1: 4 or 8 mm slicing in a horizontal plane; Plane 2: 8 mm slicing in a vertical plane perpendicular to board length and Plane 3: 8 mm slicing in a vertical plane parallel to the board length. This combined sufficient image detail quality with reasonable imaging time. The MRI system used in the experiment with the WPC experimental board prepared for imaging is shown in Figure 4. It was expected that only free water above the fibre saturation point in the wood, which was our primary interest, would be visible on the image in the form of brighter areas due to the relatively long signal



Figure 4. MRI system used for imaging the presence of water in the WPC boards.

lifetime of mobile water. For this reason, imaging of the frozen samples was avoided.

Results

Characterization of the WPC boards

Testing of the experimental and commercial WPC boards showed that they had densities of 1.14 g/cm³ and 1.09 g/cm³, respectively. Table II shows the WA and MC of the boards with respect to their total water uptake from storage and 24 hour water immersion. Table II also shows the WA after 24 hour water immersion only, expressed as an overall percentage and as the amount of water having entered the composite during the 24 hour water immersion per square centimetre (or square inch) of its exposed WPC surface. As mentioned above, this latter calculation was to account for the presence of capping between the experimental and commercial boards. WA differences during the long storage of WPC boards cannot be practically compensated by conditioning of the samples prior to testing due to their very slow water absorption/desorption (drying) process contrary to that of solid wood. The WA and MC of Western Maple solid wood, as well as polyethylene, at identical test conditions are also provided in Table II for comparison purposes.

Figures 5 and 6 provide CT images of the experimental and commercial board samples, respectively. Figures 5a and 6a show the 3D reconstructed volume of the samples, annotated with the plane indicating where the subsequent 2D image was

obtained. All 2D images were obtained in the extrusion direction and near the centre of each sample. Figures 5c and 6c show higher magnification views of the extrusion cross-section of each sample. The average volume percentages of voids for the experimental and commercial WPC samples were 1.0% and 0.5%, respectively (Table III).

Analysis of the commercial WPC board showed that there was also 58.2% wood flour blended with thermoplastic resin that was identified as polyethylene from the FTIR spectrum (Figure 7) and DSC thermogram (Figure 8). The DSC thermogram showed resin-melting temperature peaks of 109.2°C and 125.2°C. This established that the polyethylene was a blend of low-density and linear low-density resins. The protective coating that appeared only on the upper side of the board had 1.11 mm average thickness and was analysed separately with respect to resin characterization. FTIR and DSC analysis (Figure 7 and 8) classified this resin as a high-density polyethylene with a melting temperature of 134.7°C, blended with other unidentified materials.

The wood flour particles used in the commercial WPC had an average particle surface size of 0.029 mm². The particle size distribution is shown in Figure 9. The aspect ratio of wood fibre was measured as 3.31. It should be mentioned that the particle size measurements applied to the final product manufactured by extrusion, not to the raw material used for the process. Fibre size can frequently be reduced during extrusion.

The ash content of the commercial board sample was 1.25% at 675°C and less than 0.1% at 900°C.

Table II. Characterization of solid wood, experimental and commercial WPC and polyethylene.

Material	Wood content (%)	Density ^a (g/cm ³)	Total water uptake from storage ^b		Total water uptake from storage and 24-hour water immersion ^b		WA from 24-hour water immersion only ^b	
			WA ^c (%)	MC ^c (%)	WA ^c (%)	MC ^c (%)	Overall (%)	Per exposed area ^d (g/cm ²) [g/inch ²]
Solid wood ^e	100	0.45	11.01	11.01	31.84	31.84	20.83	0.0924 [0.5960]
Experimental ^f WPC	67.0	1.14	3.37	5.03	4.31	6.43	0.94	0.0099 [0.0636]
Commercial WPC	58.2	1.09	0.48	0.82	1.10	1.89	0.62	0.0091 [0.0589]
Polyethylene	0	0.92	0.00	N/A	0.02	N/A	0.02	0.0000

^aMeasured using oven-dried samples (103°C for 2 days).

^bDetermined as per ASTM D7031/D1037.

^cWA is the water mass in the WPC sample while MC is calculated as the water mass divided by the wood content.

^dCalculated as the amount of water having entered the composite during 24-hour water immersion per square centimetre (or square inch) of its WPC-exposed surface.

^eWestern Maple.

^fThe water uptake properties were tested on one specimen due to the limited availability of the material; water uptake testing was done in duplicate for all other materials.

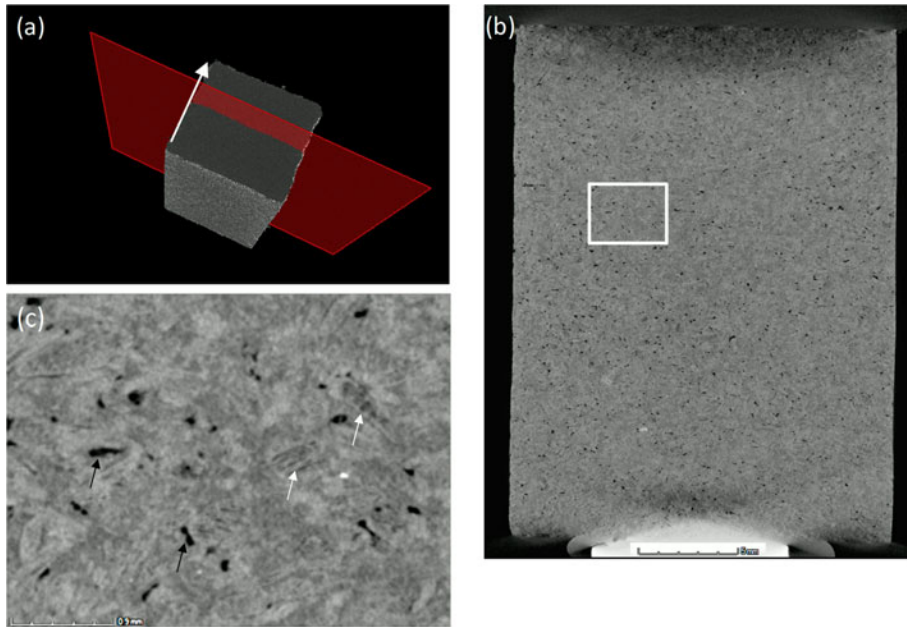


Figure 5. CT images taken in the extrusion direction of the reconstructed volume of an experimental WPC board sample with (a) plane indicator showing where the image was obtained with arrow indicating extrusion direction, (b) overview image with annotated area of focus for (c) higher magnification view of voids and wood particles present, with a black arrow indicating examples of voids and white arrows indicating examples of wood flour particles likely containing micro-voids.

MRI of the experimental WPC board

For the experimental WPC board, a total of four magnetic resonance (MR) images (slices) were taken in a horizontal plane (Plane 1), 10 in a plane perpendicular to the board length (Plane 2) and 10 in a plane parallel to the board's length (Plane 3)

(Figure 3). Select MR images for these three planes are presented in Figures 10–12, respectively. Figures 10a, 11a and 12a show the respective overviews of the slices obtained in each of the evaluated planes to serve as a reference for the location of the slices shown in the other images.

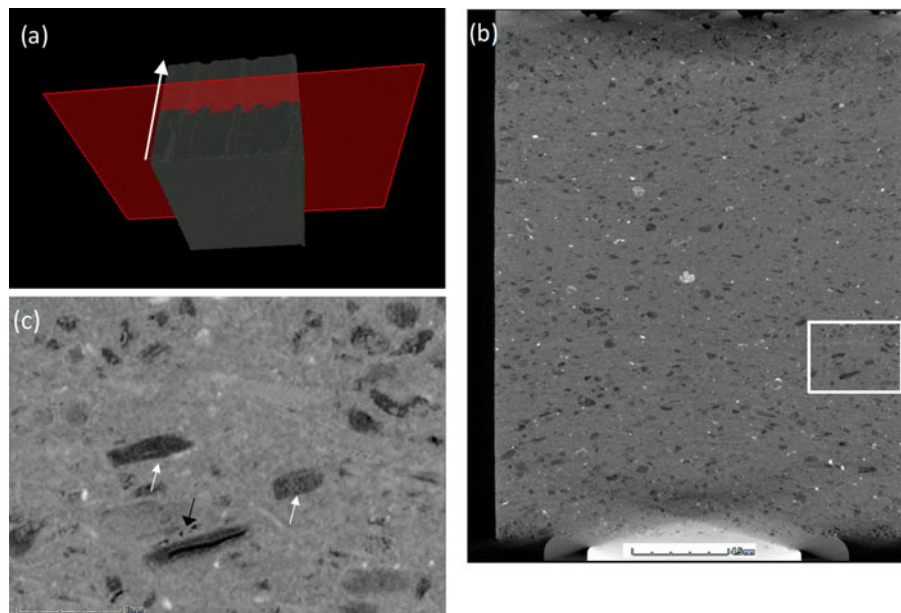


Figure 6. CT images taken in the extrusion direction of the reconstructed volume of a commercial WPC board sample with (a) plane indicator showing where the image was obtained with arrow indicating extrusion direction, (b) overview image annotated with area of focus for (c) higher magnification view of voids and wood particles present, with a black arrow indicating examples of voids and white arrows indicating examples of wood flour particles likely containing micro-voids.

Table III. Void analysis of experimental and commercial WPC samples based on CT.

Material	Void volume (%)		Detected volume ranges (mm ³)
	Average ^a	Standard deviation ^a	
Experimental	1.0	0.2	4.1×10^{-6} to 5.6×10^{-3}
Commercial	0.5	0.1	4.1×10^{-6} to 0.16

^aAverage of three sub-volumes tested.

Figures 13 and 14 present magnified images of select slices from Planes 3 and 2, respectively, which have been annotated to show the depth of water penetration above wood fibre saturation.

To further analyse free water distribution in the exposed experimental WPC board, samples were cut, wafered, and dried to measure the WA and MC distribution within the board area of interest as described in the section ‘Destructive Testing for WA and MC’. The results of this testing are shown in Figures 15–17. Each of these figures has been combined with the corresponding segments of MR images to directly compare the bright portion of the image with the water detected in the sample using the destructive testing method.

MRI of the commercial WPC board

For the commercial WPC board, a total of 7 MR images were taken in a horizontal plane (Plane 1), 10 in the plane perpendicular to board length (Plane 2) and 10 in the plane parallel to board length (Plane 3) (Figure 3). Figures 18–20 show the MR images for select slices obtained from Planes 1, 2 and 3, respectively. Figures 18a, 19a and 20a show an

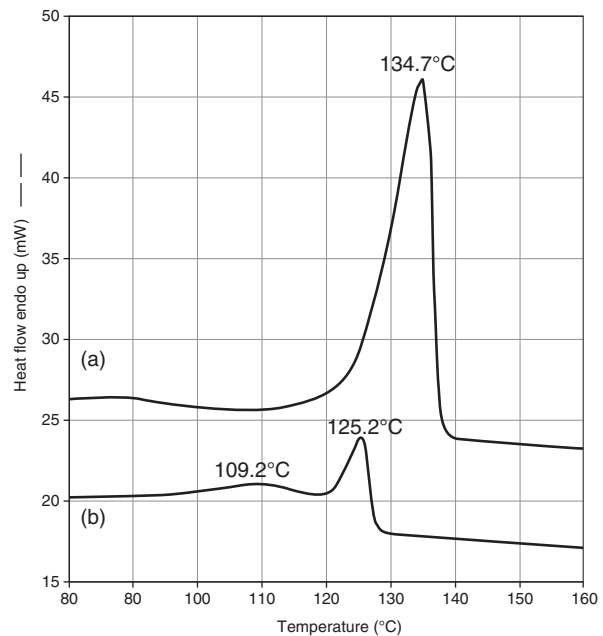


Figure 8. DSC thermograms of (a) commercial board protective coating and (b) WPC composite material.

overview of the slices obtained in each of the evaluated planes to serve as a reference for the location of the slices shown in the other images. A magnified image of Plane 3 Slice 4 with measurements indicating the presence of above wood fibre saturation is presented in Figure 21.

Discussion

WA and MC

The polyethylene had very low WA (0.02%) during the 24 hour water immersion experiment, which was

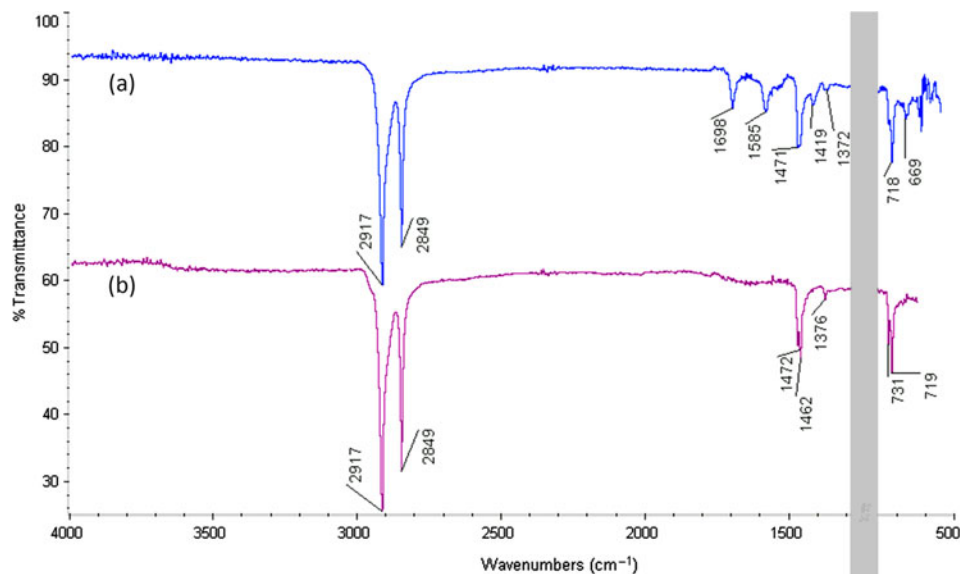


Figure 7. FTIR spectra of (a) commercial board protective coating and (b) resin from WPC polymer matrix.

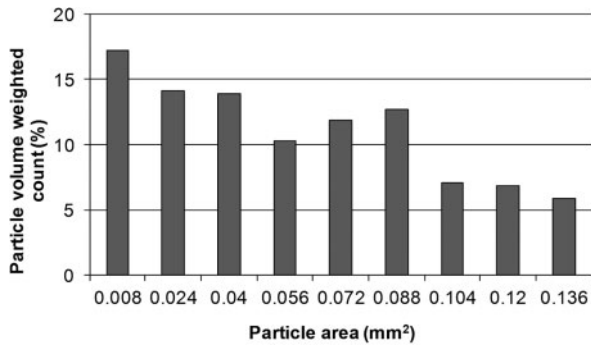


Figure 9. Wood particle size distribution in wood flour recovered from commercial WPC board.

expected. This could explain the limited commercial board WA (1.10%) and MC of the wood in the composite (1.89%), which was observed during testing (Table II). Also, it could be expected that all water in the composite detected by MRI would be only present in the fine wood flour. WA and MC of solid wood measured at the same conditions were significantly higher (31.8%), as shown in Table II. The WA and MC of the experimental board were similar to the commercial product, when its longer storage and its lack of a water-impervious protective coating were taken into consideration. In this case, calculated WA values of the experimental and commercial composite were almost identical at 0.0099 g/cm² and 0.0091 g/cm² (0.0636 g/in² and 0.0589 g/in²), respectively.

Microstructure and voids

Voids, as indicated by black spots, can be seen interspersed throughout the experimental sample (Figure 5), whereas in the commercial sample there were fewer voids (Figure 6). Assumptions were made that the theoretical wood density (without any voids) is 1.4 g/cm³ and that polyethylene densities in the experimental and commercial boards are 0.955 and 0.920 g/cm³, respectively. The density effects of the small amount of additives present in both samples were assumed to be negligible and not taken into consideration. Based on these assumptions and the densities and wood content of the tested boards presented in Table II, the total voids volume could be estimated as 6.0% and 5.2% for the experimental and commercial WPCs, respectively. When the amount of voids larger than 4.1×10^{-6} mm³ as detected by the CT instrument is subtracted, 1.0% for the experimental WPC and 0.5% for the commercial WPC, this leaves approximately 5.0% and 4.7% volume of micro-voids unaccounted for in each respective material. It is reasonable to expect that the majority of these micro-voids are

associated with empty lumens in wood flour particles, which were not completely filled with polymer. This could be seen as darker grey features on the micro X-ray CT photographs (Figures 5 and 6). Such micro-voids could potentially become major free water storage reservoirs, with their total volume approximately 5–10 times larger than the volume of larger voids present as detected by the CT data.

MRI of the experimental WPC board

Figures 10 to 12 show sharp bright borders along the board edges where the majority of the absorbed free water was present. The measurements, based on the external bright border of the sample, taken from Figure 10a confirmed the physical size of the board dimensions with good accuracy. The board width and thickness measured by MRI image analysis on Figure 10a was 143.5 mm (5.65") and thickness 27.5 mm (1.08"), respectively, while the width and thickness of the exposed, wet board measured directly with a calliper was 143.3 mm (5.67") and 27.5 mm (1.10"), respectively. A similar bright border which indicated the presence of free water above wood fibre saturation can be seen in the images obtained in Plane 2 Slice 8 taken in the middle between the exposed end and the support (Figure 11b).

Separate attention was required for the MR images in the area of the board support that had a significantly larger bright area which propagated towards the board centre, as well as for the exposed end of the board, which also showed increased WA in the form of a bright pronounced area. As shown in Figures 12 and 13a, the board support area seemed to be the largest factor in water entry for the WPC decking. The zone with MC around 25% and above in this area penetrated to about 15.5 mm (0.61") from the board bottom surface in a semi-elliptical shape. This maximum, as expected, was in the middle of the 38 mm wide support. It is also interesting that the zone with increased MC was not only limited to direct contact of the board with the support but also significantly extended to span over 64 mm (2.52"). The MR image also indicated that only 9 mm (0.35"), which was about 35% of the board cross-section in this area, had MC below the fibre saturation point. Due to the shape of the moisture distribution, very limited information with respect to the range of moisture increase of the WPC board in contact with the support could be obtained from destructive testing. This increase of MC in the WPC board in the area of the support could be easily explained by the mass transfer phenomenon associated with limited water drying in this area, combined with the easy entry of water along the WPC board and the support interface. This phenomenon

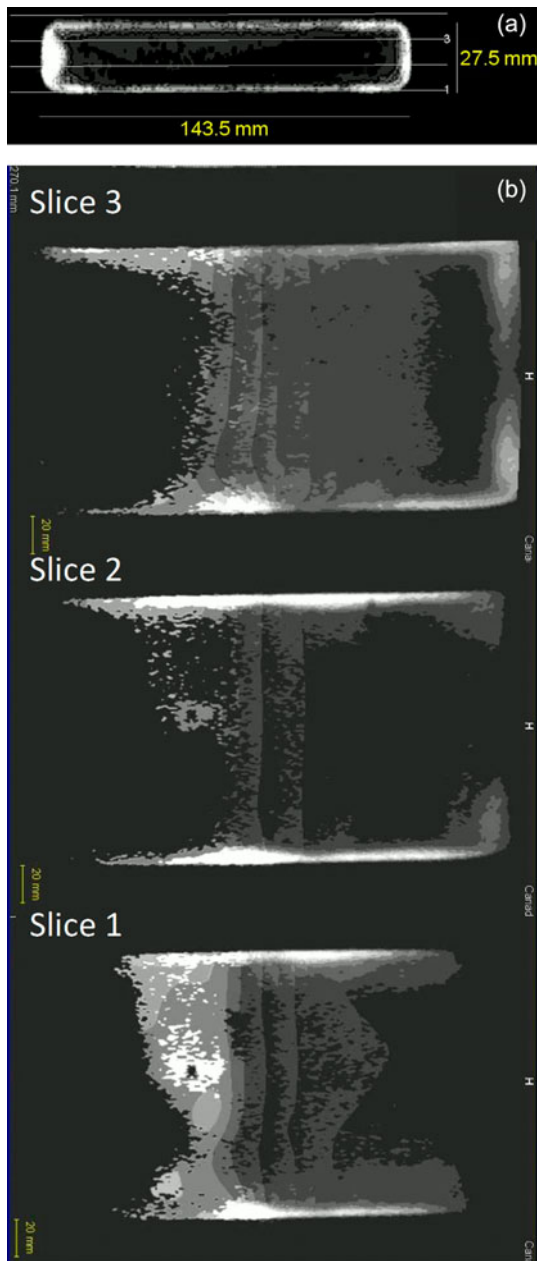


Figure 10. MR images of experimental WPC board #106 obtained in Plane 1 with (a) slice locator and (b) selected Slices 1, 2 and 3 in this plane (horizontal). Note the board dimension measurements obtained using the MRI software measuring tool.

also occurs frequently in solid wood structures, causing significant decay damage. Also of interest was a visible dark shadow in the centre of the board in Figure 13a which matched the location of a hole drilled in this place for a fastening screw. No significant increase of MC around this location during exterior exposure was detected. Only some limited increase in MC, in the form of a brighter spot on the side of the darker shadow that is the image of the empty screw hole, can be seen in the MR image. This brighter spot could also be

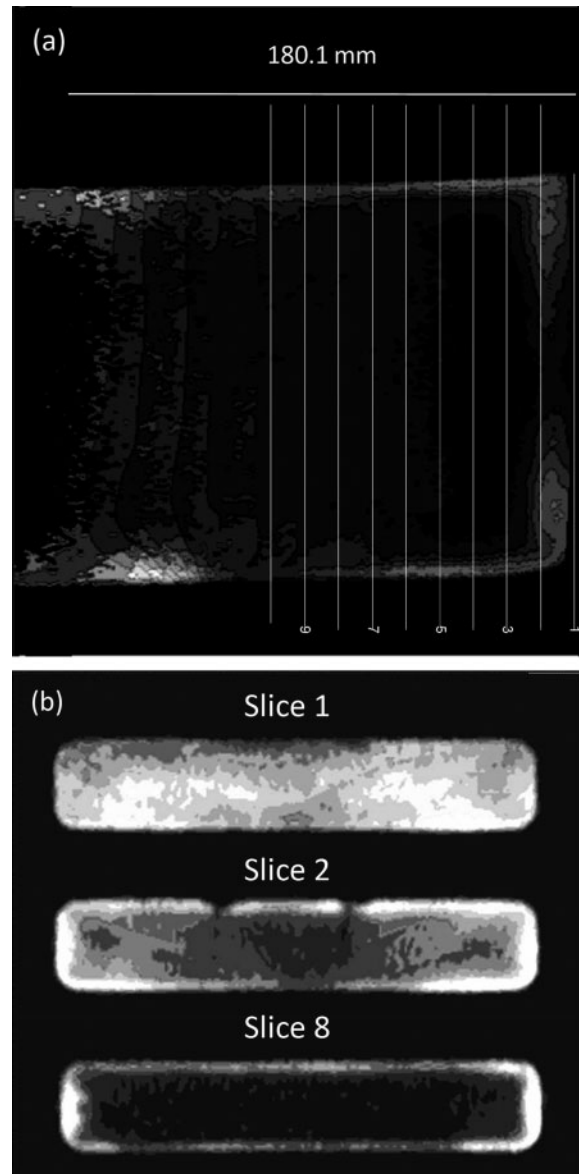


Figure 11. MR images of experimental WPC board #106 obtained in Plane 2 with (a) slice locator and (b) selected Slices 1, 2 and 8 in this plane (perpendicular to the board length direction).

explained by the tight contact between the board and the support beam in this area.

The sides of the board were another place that was identified as being sensitive to water entry in the composite. The cut end was particularly sensitive to moisture absorption (Figure 13b). Here, the MC zone that exceeded the fibre saturation point in wood ranged about 15 mm, regardless of the fact that this end was freely suspended in the air without the presence of factors that may have contributed to increased water uptake. Some explanation of this phenomenon could be the wood fibre orientation associated with the extrusion process and the expected preferred direction of moisture migration along these fibres.

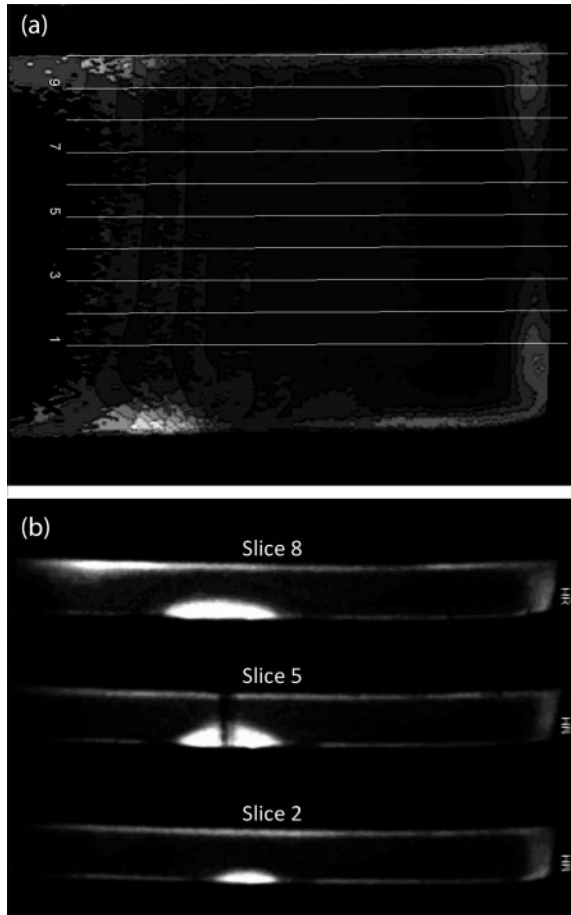


Figure 12. MR images of experimental WPC board #106 obtained in Plane 3 with (a) slice locator and (b) selected Slices 2, 5 and 8 in this plane (parallel to the board length direction).

The increase in the depth of water penetration significantly above fibre saturation could be seen along the sides of the board in the middle of the

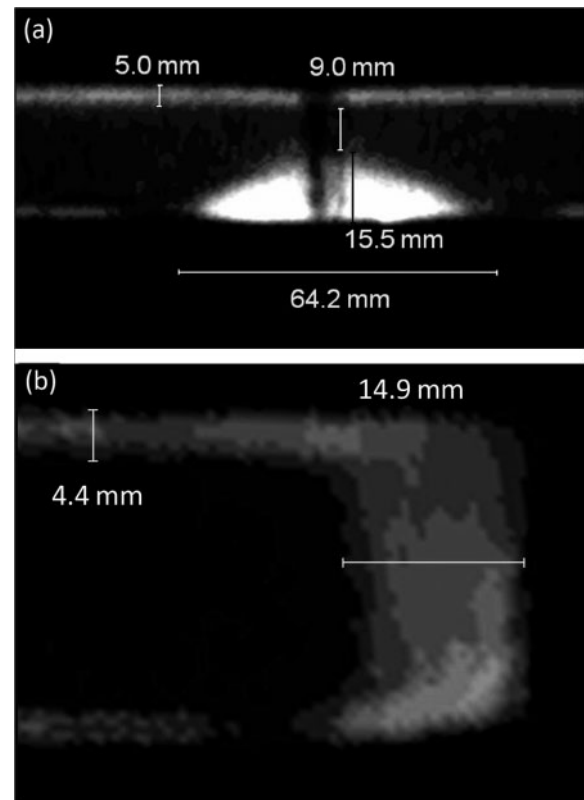


Figure 13. (a) Magnified area of the board support visible in Plane 3 Slice 5 with measurements indicating water presence above wood fibre saturation and (b) magnified area of cut end of the board visible in Plane 3 Slice 2 with measurements indicating water presence above wood fibre saturation.

board thickness to about 10 mm (0.39") as shown in Figure 14. This water distribution pattern could not be fully explained at this point and may be related to the composite porosity present in this region due to extrusion stresses or other related conditions.

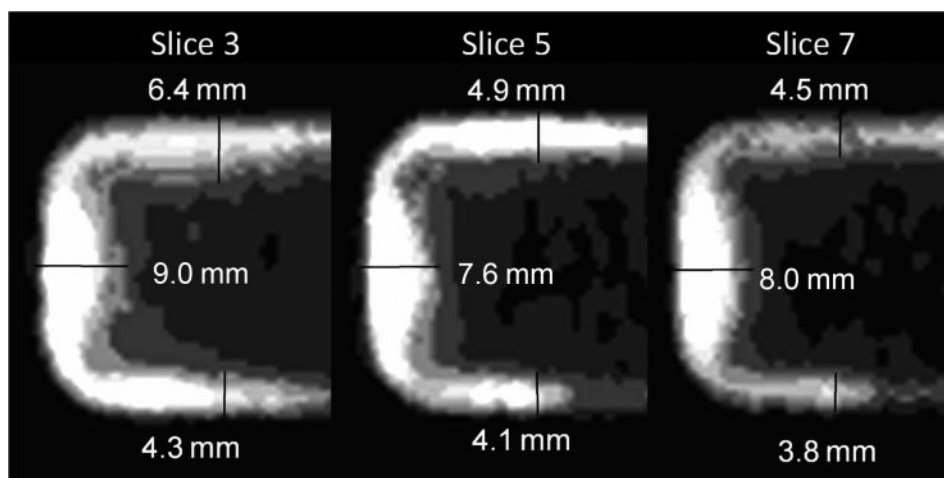


Figure 14. Magnified MR images of Plane 2 selected Slices 3, 5 and 7 from the side of the experimental WPC board #106 with measurements indicating the depth penetration of water above wood fibre saturation.

Both the upper and lower board surfaces also showed the presence of MC exceeding the fibre saturation point in wood. The zones with this MC were about 4–6 mm (0.16–0.24") in thickness on both the upper and lower sides of the tested board as can also be seen in Figure 14. In particular, an increase in MC at the bottom of the board is visible along the ‘dripping edge’ where rain or dew water has a tendency to be present for a prolonged period of time in the form of hanging droplets.

Comparison of MR images of experimental board with destructive testing results

As shown in Figures 15–17, the bright part of the image became grey and began to disappear, matching the black background around the point where the MC in wood reached 22–24%. This is particularly visible in Figure 16 and part of Figure 17, where water diffusion occurs in only one direction, along the vertical plane. This indicated that the moisture saturation point was most likely reduced in the

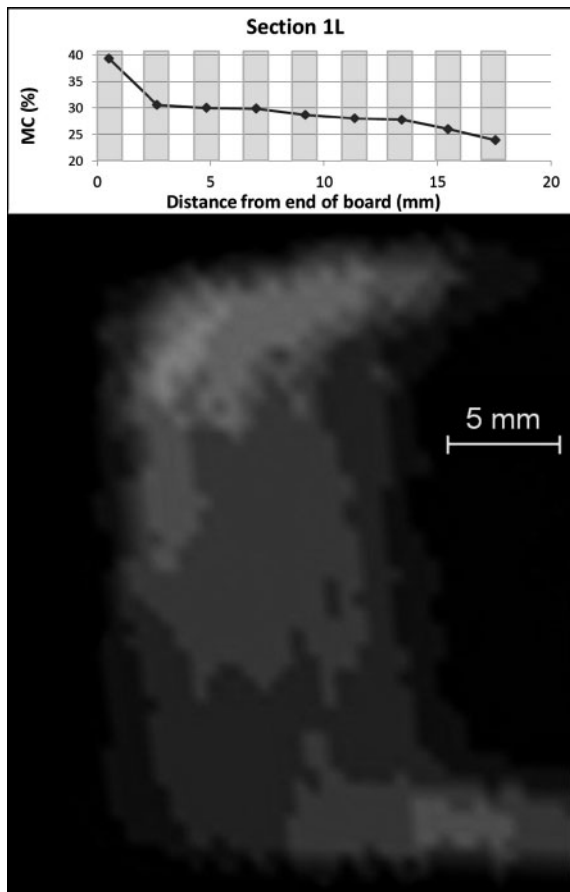


Figure 15. MC of wood found in the experimental board cross-section 1L around the cut edge with distance from the board end in comparison to an MR image of this area (Plane 3 Slice 2). The shaded areas on the graph indicate the location and thickness of individual wafers used for destructive MC testing.

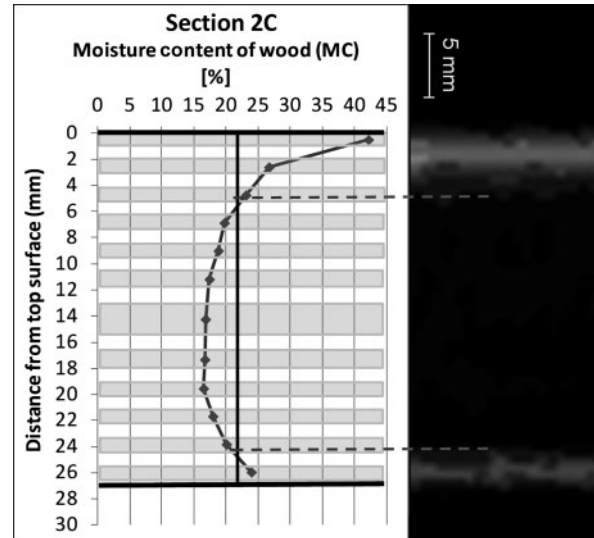


Figure 16. MC of wood found in the experimental board cross-section 2C with distance from the exposed board surface in comparison to an MR image of this area (Plane 3 Slice 5). Approximately 22% MC, which is around the wood fibre saturation point, is marked on the graph. The shaded areas on the graph indicate the location and thickness of individual wafers used for destructive MC testing.

composite wood flour particles by about 5% as typical fibre saturation occurs for most solid wood species at MC of about 25–30%. In general, there is a good correlation between MR images and MC measured by destructive testing involving drying of the samples taken. This experiment confirmed the expectation that water in WPC could be effectively

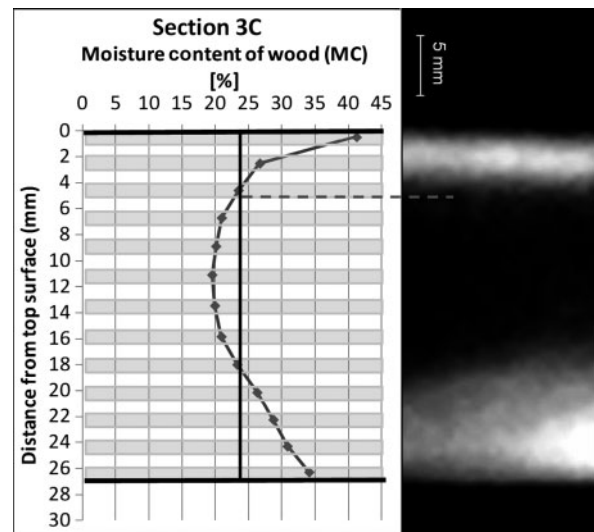


Figure 17. MC of wood in section 3C at board support with distance from the exposed board surface in comparison to an MR image of this area (Plane 3 Slice 5). Approximately 24% MC, which is around the wood fibre saturation point, is marked on the graph. The shaded areas on the graph indicate the location and thickness of individual wafers used for destructive MC testing.

detected by MRI at a concentration close to fibre saturation or above it using a clinical MRI unit.

The grey areas of all the MR images seemed to quickly disappear and transform into relatively bright white areas around MC 30% in the tested board. Researchers successfully used a transmission densitometer on MR images to directly measure the moisture gradient and/or distribution within the wood (Olson *et al.* 1990). Due to the relatively sharp transition from the grey areas of the images into relatively bright, almost white fields in the narrow MC range between 25% and 30% in the WPC board, measurement of the MC value on the images was omitted in our work.

Knowledge about water distribution and wood fibre saturation is very important from a material durability point of view as fibre saturation point at about 25% MC in wood, including wood in a composite material, can be treated as an initiation point where decay fungi become active in cellulose and lignin decomposition as was mentioned earlier. Surpassing this threshold is an indication that the board, or at least a portion of it, may become damaged by the decay process during exterior exposure. The obtained MR images of the experimental WPC board exposed to exterior conditions confirmed details of the complex moisture gradient between the exterior surface and the board core. The

effects of exterior exposure as imaged by MRI relating to the presence of water in the composite decking boards seem to contradict the low WA results obtained during characterization of the material.

MRI of commercial WPC board

The pattern of water entry in the commercial WPC board imaged after exposure near Hilo, Hawaii, for 2 years (Figures 18–21) was similar to that found earlier in experimental composite board #106. The exception was the upper board surface, where no brighter image associated with presence of water was detected. This surface was covered by a coextruded polyethylene coating (capping), which seemed to be very effective in protecting the WPC board body against moisture entry into the upper board surface. The location of this protective coating, not always well visible on the MR images, has been marked with a dashed line. There were, however, signs of significant vulnerability of this board to water entry at other places. At the support area, MC above the fibre saturation point in wood measured almost 7 mm (0.28") in comparison to only up to 2 mm (0.08") along the lower surface as shown in Figure 21a and b, respectively, despite only 2 years of exterior exposure for this sample.

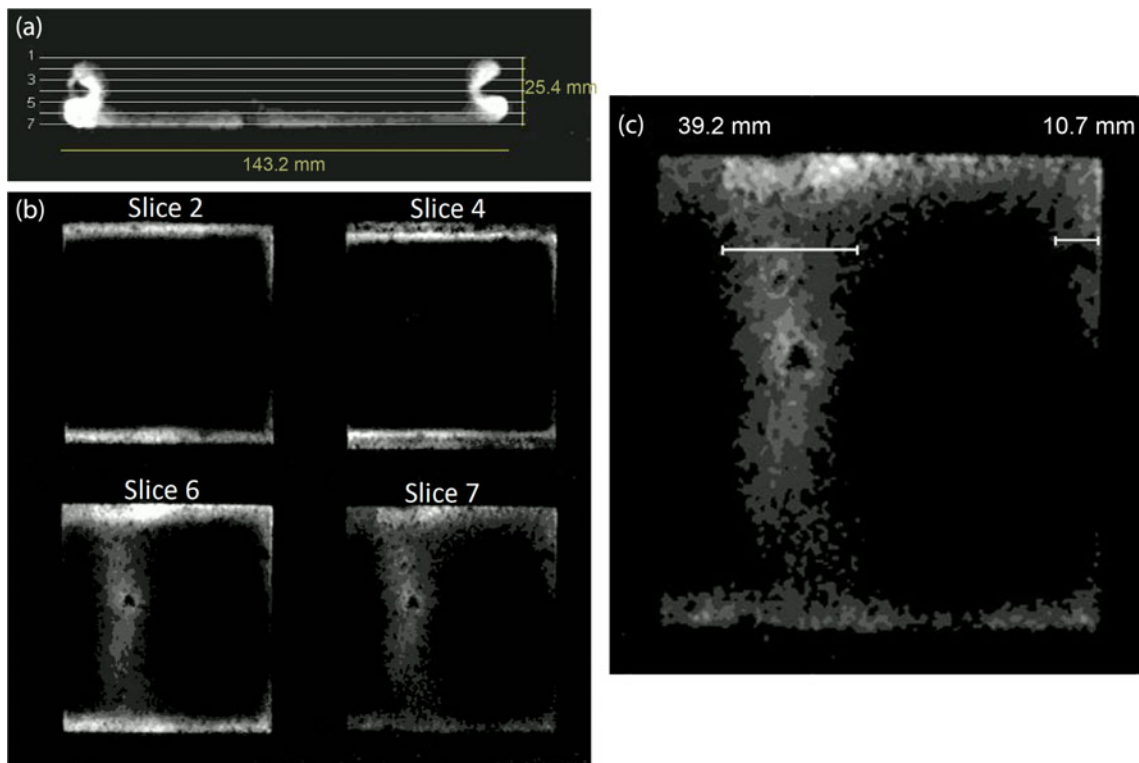


Figure 18. MR images of the commercial WPC board obtained in Plane 1 with (a) slice locator, (b) selected Slices 2, 4, 6 and 7 in this plane (horizontal) and (c) magnification of Slice 6 with measurements indicating water presence above wood fibre saturation.

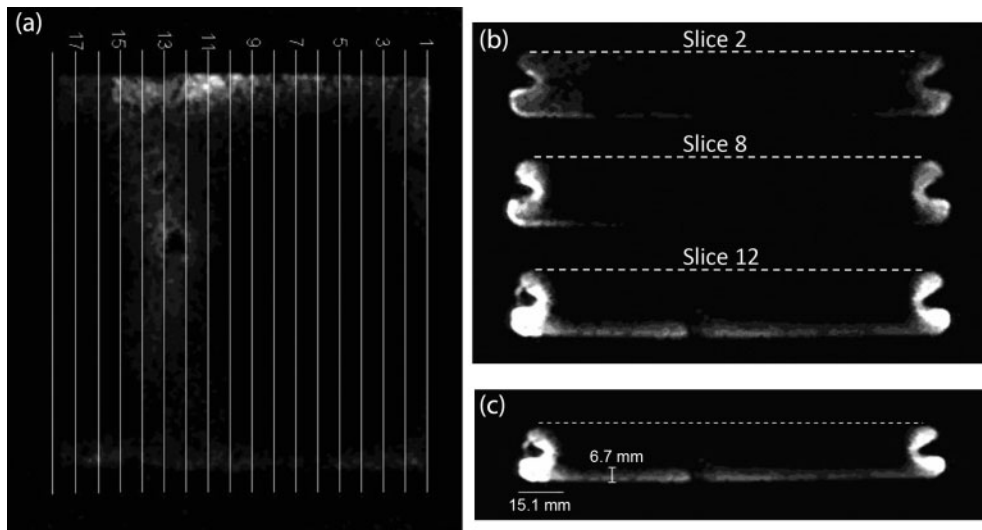


Figure 19. MR images of the commercial WPC board obtained in Plane 2 with (a) slice locator, (b) selected Slices 2, 8 and 12 in this plane (perpendicular to the board length) and (c) magnification of Slice 12 with measurements indicating water presence above wood fibre saturation. The dotted lines in (b) mark the edges of the board protected by the extruded coating.

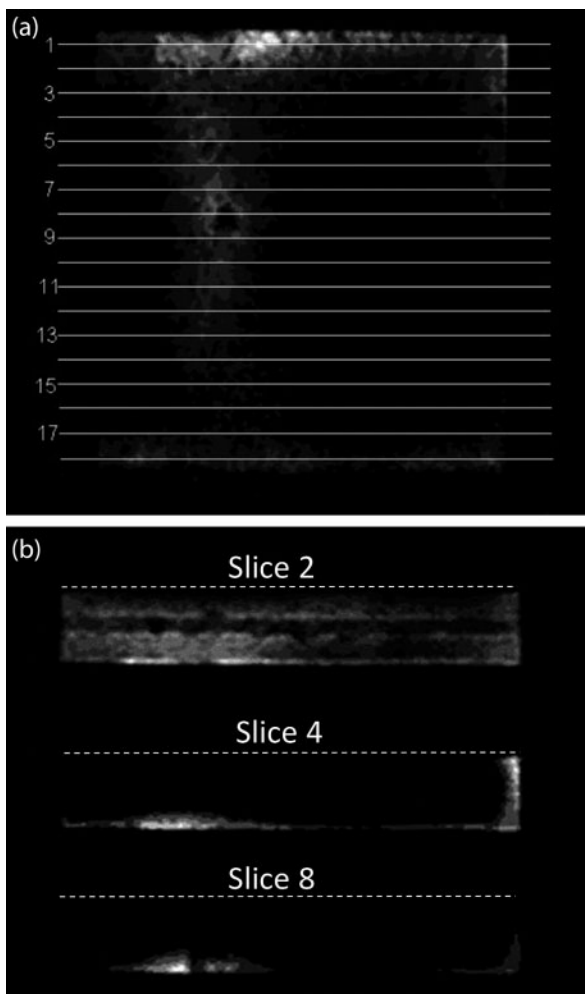


Figure 20. MR images of commercial WPC board obtained in Plane 3 with (a) slice locator and (b) selected Slices 2, 4 and 8 in this plane (vertical and parallel to the board length). The dotted lines in (b) mark the edges of the board protected by coating.

Furthermore, there was a large water entry area associated with the board's fastening grooves with accumulation of free water from the exposed side up to a distance of about 15 mm (0.59"). This aggressive water entry could be seen extending into the area covered by the coextruded coating as shown in [Figure 19](#). Partial entry of water under the coextruded coating may have created an accumulation of water in this area due to the reduced possibility of evaporation. This WA around the grooves was present all along the tested board segment.

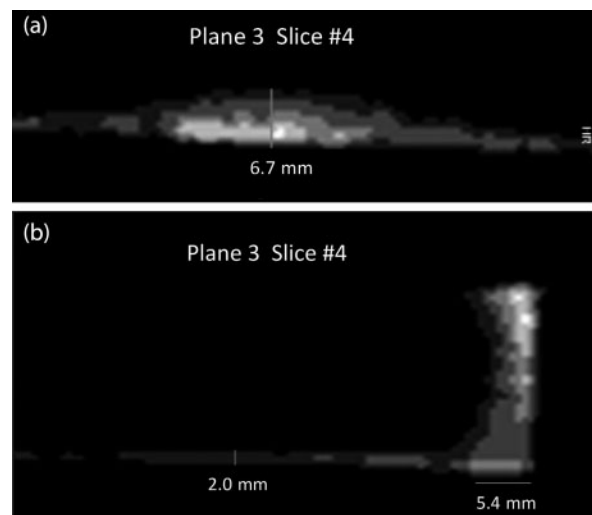


Figure 21. Magnification of an MR image of the commercial WPC board in (a) Plane 3, Slice 4 in the area of the board support and (b) Plane 3 Slice 4 in the area of the board cut end, both with measurements indicating water presence above fibre saturation point.

As could be expected, there was also significant WA at the cut end of the board as shown in Figure 21b. The penetration depth of excessive MC above the wood fibre saturation point was variable along the surface, with a large region around board edges assessed at about 6 mm (0.24"). Note that this end of the board was cut 1 year earlier for another purpose, prior to the tested sample collection. The cut end of the board and the support area together with the grooved board seemed to be the most vulnerable water point of entry as identified by MRI. It would be very difficult to protect this area, and additional accumulation near the edges may occur due to evaporation being obstructed by the coating.

Conclusions

The results presented demonstrate that MR images can be used successfully for the detection of free water above wood fibre saturation in WPC boards. It was confirmed that this technique allowed for a non-destructive, detailed water entry analysis around 25% MC and with 4 to 8 mm MRI acquisition slice thickness. Details such as the location where a fastening screw had once been were visible. Results from analysis of the MR images were confirmed by destructive sampling and testing of MC in imaged WPC boards by the conventional drying process. Further examination of the obtained MR images allowed for the identification of details of MC distribution in exterior WPC decking boards. Major points of water entry seemed to be the board support point and exposed cut ends, which are present in a significant number of capped WPC decking boards. Sensitivity to moisture entry around the extruded fastening grooves on the side of the board was also identified. Increased MC was also found on the MR images along the 'dripping edge' of the board and in the upper board surface if it was not protected by capping.

MRI indicated approximately 22–24% MC in the experimental board. This indicated that the fibre saturation point was most likely reduced in the composite wood flour particles by about 5% as typical fibre saturation occurs for most solid wood species at MC of about 25–30%. There was also significant water content above fibre saturation detected in the commercial board, likely also around 25%. Since the decay of wood in WPC could be initiated at the fibre saturation point, MRI could be an appropriate tool in evaluating WPC durability in this respect. Also, mechanical properties of composites are known to be greatly affected by the presence and distribution of water, and this distribution should be taken into consideration during testing. Due to the irregular shape of some moisture

distributions, details of this analysis would be difficult to achieve using the conventional destructive methods. Water content and distribution analysed from MRI was compared with the destructive method of MC measurement and showed a good correlation. These results may be helpful in designing WPC boards designated for exterior exposure with reduced or possibly eliminated water entry into the product.

Acknowledgements

The authors would like to thank Irene Kinoshita of Canadian Magnetic Imaging Laboratory for her assistance, advice and MRI samples of WPC boards. The authors would also like to thank GE Inspection Technologies, LP for the use of their phoenix|X-ray nanotom m, and Dr Meghan Faillace, lead applications engineer for GE Inspection Technologies, LP for her assistance, expertise and CT imaging of the WPC materials.

References

- Araujo, C. D., McKay A. L., Hailey J. R. T. and Whittall, K. P. (1992) Proton magnetic resonance techniques for characterization of water in wood: Application to white spruce. *Wood Science Technology*, 26, 101–113.
- ASTM International (2013a) *ASTM Standard D9–12, Standard Terminology Relating to Wood and Wood-Based Products* (West Conshohocken, PA: ASTM International), 12 pp.
- ASTM International (2013b) *ASTM Standard D1037–12, Standard Test Methods for Evaluating Properties of Wood-Base Fiber and Particle Panel Materials* (West Conshohocken, PA: ASTM International), 31 pp.
- ASTM International (2013c) *ASTM Standard D7032–10a, Standard Specification for Establishing Performance Ratings for Wood-Plastic Composite Deck Boards and Guardrail Systems (Guards of Handrails)* (West Conshohocken, PA: ASTM International), 11 pp.
- ASTM International (2013d) *ASTM Standard D7031–11, Standard Guide for Evaluating Mechanical and Physical Properties of Wood-Plastic Composite Products* (West Conshohocken, PA: ASTM International), 8 pp.
- Bucur, V. (2003) *Nuclear Magnetic Resonance in Nondestructive Characterization and Imaging of Wood* (Berlin: Springer-Verlag), pp. 215–279.
- Cheng, Q., Muszynski, L., Shaler, S. and Wang, J. (2010) Microstructural changes in wood plastic composites due to wetting and re-drying evaluated by X-ray microtomography. *Journal of Nondestructive Evaluation*, 29, 207–213.
- Clemons, C. M. and Ibach, R. E. (2002). Laboratory tests on fungal resistance of wood filled polyethylene composites. In *Proceedings of ANTEC, May 5–9, 2002, San Francisco, CA* (Newtown, CT: Society of Plastics Engineers), pp. 2219–2222.
- Clemons, C. M. and Ibach R. E. (2004) Effects of processing method and moisture history on laboratory fungal resistance of wood-HDPE composites. *Forest Products Journal*, 54, 50–57.
- Defoirdt, N., Gardin, S., Van den Bulcke, J. and Van Acker, J. (2010) Moisture dynamics of WPC and the impact on fungal testing. *International Biodeterioration & Biodegradation*, 64, 65–72.
- Englund, K. and Olson, B. (2007) Processing influences on wood-plastic composite properties – Extrusion screw speed.

- In *Proceedings of the 9th International Conference on Wood & Biofibre Plastic Composites, Madison, WI*, pp. 87–91.
- Evans, P. D., Morrison, O., Senden, T. J., Vollmer, S., Roberts, R. J., Limaye, A., Arns, C. H., Averdunk, H., Lowe, A. and Knackstedt, M. A. (2010) Visualization and numerical analysis of adhesive distribution in particleboard using X-ray micro-computed tomography. *International Journal of Adhesion and Adhesives*, 30, 754–762.
- Gacitua, W., and Wolcott, M. (2009) Morphology of wood species affecting wood-thermoplastic interaction: Micro-structure and mechanical adhesion. *Maderas, Ciencia y tecnologia*, 11, 217–231.
- Gnatowski, M. 2005. Water absorption by wood-plastic composites in exterior exposure. In *Proceedings of the 8th International Conference on Woodfibre-Plastic Composites, Madison, WI*, pp. 249–256.
- Gnatowski, M. 2009. Water absorption and durability of wood-plastic composites. In *Proceedings of the 10th International Conference on Wood & Biofibre Plastic Composites and Cellulose Nanocomposites Symposium, Madison, WI*, pp. 90–102.
- Hall, L. D., Rajanayagam, V., Stewart, W. A. and Steiner, P. R. (1986) Magnetic resonance imaging of wood. *Canadian Journal of Forest Research*, 16, 423–426.
- Ibach, R. E. and Clemons, C. (2002) Biological resistance of polyethylene composites made with chemically modified fibre or flour. In P.E. Humphrey (ed.) *6th Pacific Rim Bio-Based Composites Symposium, Oregon State University, Portland, OR*, pp. 574–583.
- Kastner, J., Plank, B. and Salaberger, D. (2012) High resolution X-ray computed tomography of fibre- and particle-filled polymers. In *18th World Conference on Nondestructive Testing, Durban, South Africa*, pp. 16–20.
- Lulianelli, G., Tavares, M. B. and Luetkmeyer, L. (2010) Water absorption behaviour and impact strength of PVC/wood flour composites. *Chemistry and Chemical Technology Journal*, 4, 225–229.
- Jin, X., van der Sman, R. G. M., Gerkema, E., Vergeldt, F. J., van As, H. and van Boxtel, A. J. B. (2011) Moisture distribution in broccoli: Measurements by MRI hot air drying experiments. In *11th International Congress on Engineering and Food (ICEF11)*, *SciVerse Science Direct, Procedia Food Sciences*, 1, 640–646.
- Jones, M., Aptaker, P. S., Cox, J., Gardiner, B. A. and McDonald, P. J. (2012) A transportable magnetic resonance imaging system for *in situ* measurements of living trees: The Tree Hugger. *Journal of Magnetic Resonance*, 218, 133–140.
- Jördens, C., Wietzke, S., Scheller, M. and Koch, M. 2010. Investigation of the water absorption in polyamide and wood plastic composite by terahertz time-domain spectroscopy. *Polymer Testing*, 29, 209–215.
- Kaboorani, A., Cloutier, A. and Wolcott, M. P. (2007). Effects of water absorption on mechanical properties of high-density polyethylene wood composites. In *Proceedings of the 9th International Conference on Wood & Biofibre Plastic Composites, Madison, WI*, pp. 175–183.
- Korte, H. and Hansmann, H. 2005. Wood-plastic composites made with different processes: A comparative investigation. In *Proceedings of the 8th International Conference on Woodfibre-Plastic Composites, Madison, WI*, pp. 51–55.
- Laks, P. E., Richter, D. L., Larkin, G. M. and Eskola, J. O. (2010) A survey of the biological resistance of commercial WPC decking. In *10th Pacific Rim Bio-based Composites Symposium*, pp. 193–201.
- Laks, P., Vehring, K., Verhey, S. and Richter, D. (2005) Effect of manufacturing variables on mold susceptibility of wood-plastic composites. In *Proceedings of the 8th International Conference on Woodfibre-Plastic Composites, Madison, WI*, pp. 265–270.
- Laks, P. E. and Verhey, S. A. (2000) Decay and termite resistance of thermoplastic/wood fibre composites. In P. D. Evans (ed.) *Proceedings, 5th Pacific Rim Bio-Based Composites Symposium, Department of Forestry, The Australian National University, Canberra, Australia*, pp. 727–734.
- MacMillan, B., Veliyulin, E., Lamason, C. and Balcom, B. J. (2011) Quantitative magnetic resonance measurements of low moisture content wood. *Canadian Journal of Forest Research*, 41, 2158–2162.
- Mankowski, M., and Morrell, J. J. (2000) Patterns of fungal attack in wood-plastic composites following exposure in a soil block test. *Wood Fiber Science*, 32, 340–345.
- Manning, M. J. and Ascherl, F. (2007) Wood-plastic composite durability and the compelling case for field testing. In *Proceedings of the 9th International Conference on Wood & Biofibre-Plastic Composites, Madison, WI*, pp. 217–224.
- Morrell, J. J., Stark, N. M., Pendleton, D. E. and McDonald A.G. (2009) Durability of wood-plastic composites. In *Proceedings of the 10th International Conference on Wood & Biofibre Plastic Composites and Cellulose Nanocomposites Symposium, Madison, WI*, pp. 71–75.
- Morris, P. I. and Cooper, P. (1998) Recycled plastic/wood composite lumber attacked by fungi. *Forest Products Journal*, 48, 86–88.
- Muller, U., Bammer, R., Halmshlager, E., Stollberger, R. and Wimmer, R. (2001) Detection of fungal wood decay using magnetic resonance imaging. *Holz als Roh- und Werkstoff*, 59, 190–194.
- Olson, J. R., Chang, S. J., and Wang, P. C. (1990) Nuclear magnetic resonance imaging: A non-invasive analysis of moisture distributions in white oak lumber. *Canadian Journal of Forest Research*, 20, 586–591.
- Pendleton, D. E., Hoffard, T. A., Adcock, T., Woodward, B. and Wolcott, M. P. (2002) Durability of an extruded HDPE/wood composite. *Forest Products Journal*, 52, 21–27.
- Schmidt, E. L. 1993. Decay testing and moisture changes for a plastic wood composite. *Proceedings of the American Wood-Preservers' Association*, 89, 108–109.
- Stenstrom, S., Bonazzi, C. and Foucat, L. (2009) Magnetic resonance imaging for determination of moisture profiles and drying curves. *Modern Drying Technology*, 2, 91–142.
- Telkki, V.-V., Saunavaara, J. and Jokisaari J. (2010) Time-of-flight remote detection MRI of thermally modified wood. *Journal of Magnetic Resonance*, 202, 78–84.
- Telkki, V.-V., Yliniemi, M. and Jokisaari, J. (2013) Moisture in softwoods: Fiber saturation point, hydroxyl site content, and the amount of micropores as determined from NMR relaxation time distributions. *Holzforschung*, 67, 291–300.
- TimberTech Product Catalog* (2010) Wilmington, Ohio. (http://www.goyoders.com/docs/decking/timbertech/product_choices.pdf)
- Verhey, S. A., Laks, P. E., Richter, D. L., Keranen, E. D. and Larkin, G. M. (2003) Use of field stakes to evaluate the decay resistance of wood fibre-thermoplastic composites. *Forest Products Journal*, 53, 67–74.
- Wang, P. C. and Chang, S. J. (1986) Nuclear magnetic resonance imaging of wood. *Wood Fibre Science*, 18, 308–314.
- Wang, W. and Morrell, J. (2004) Water sorption characteristics of two wood-plastic composites. *Forest Products Journal*, 54, 209–212.
- Wang, Y., Muszynski, L., Simonsen, J. (2007) Gold as an X-ray CT scanning contrast agent: Effect on the mechanical properties of wood plastic composites. *Holzforschung*, 61, 723–730.
- Yeh, S. K. and Gupta, R. K. (2007) Effect of processing variables on water absorption by polypropylene-based wood-plastic composites. In *Proceedings of the 9th International Conference on Wood & Biofibre Plastic Composites, Madison, WI*, pp. 225–233.